Experimental Neurology 339 (2021) 113594

Contents lists available at ScienceDirect

Experimental Neurology

journal homepage: www.elsevier.com/locate/yexnr

Research paper

# Age-related loss of axonal regeneration is reflected by the level of local translation

Susan van Erp [a,*], Annemiek A. van Berkel [b], Eline M. Feenstra [a], Pabitra K. Sahoo [c], Laura J. Wagstaff [a], Jeffery L. Twiss [c], James W. Fawcett [d,e], Richard Eva [d], Charles ffrench-Constant [a]

[a] MRC Centre for Regenerative Medicine and MS Society Edinburgh Centre, Edinburgh bioQuarter, University of Edinburgh, Edinburgh, UK
[b] Department of Functional Genomics, Center for Neurogenomics and Cognitive Research (CNCR), VU University Amsterdam, De Boelelaan 1085, 1081, HV, Amsterdam, the Netherlands
[c] Department of Biological Sciences, University of South Carolina, Columbia 29208, SC, USA
[d] John van Geest Centre for Brain Repair, Department of Clinical Neurosciences, University of Cambridge, Cambridge, UK
[e] Centre for Reconstructive Neuroscience, Institute of Experimental Medicine, Czech Academy of Sciences, Prague, Czech Republic

ARTICLE INFO

*Keywords:*
Axon regeneration
Human stem cells
Local translation
Proteomics
In vitro live imaging
Axotomy

ABSTRACT

Regeneration capacity is reduced as CNS axons mature. Using laser-mediated axotomy, proteomics and puromycin-based tagging of newly-synthesized proteins in a human embryonic stem cell-derived neuron culture system that allows isolation of axons from cell bodies, we show here that efficient regeneration in younger axons (d45 in culture) is associated with local axonal protein synthesis (local translation). Enhanced regeneration, promoted by co-culture with human glial precursor cells, is associated with increased axonal synthesis of proteins, including those constituting the translation machinery itself. Reduced regeneration, as occurs with the maturation of these axons by d65 in culture, correlates with reduced levels of axonal proteins involved in translation and an inability to respond by increased translation of regeneration promoting axonal mRNAs released from stress granules. Together, our results provide evidence that, as in development and in the PNS, local translation contributes to CNS axon regeneration.

## 1. Introduction

Axonal regeneration in the central nervous system (CNS) is poor, contributing to the significant disabilities associated with traumatic and other diseases of the brain and spinal cord. There are two major underlying causes that prevent successful CNS axon regeneration. First, the extrinsic environment in the CNS after injury is inhibitory, in contrast to the PNS environment where growth-permitting circumstances are found (Chen et al., 2000; Prinjha et al., 2000; Sharp et al., 2010; Fawcett et al., 2012; Geoffroy and Zheng, 2014). Second, there is an intrinsic loss of regenerative ability in the axons as the CNS completes development and neurons start to age (Eva et al., 2012; Zou et al., 2013; Fawcett and Verhaagen, 2018). During embryonic development, axons in vivo and in vitro are able to form growth cones and extend axons after injury, but this growthpotential is gradually lost in postnatal neurons (Li et al., 1995). Similarly, human embryonic stem cell (hESC)-derived neurons show a maturation-related loss of axon regeneration potential (Koseki, 2017a; Nieuwenhuis, 2020).

Given that successful therapies to enhance CNS axon regeneration will need to address both the extrinsic and intrinsic causes of failure, research into the mechanisms that limit regeneration once development is complete is essential. An important process shown to be involved in axon outgrowth during development and in the PNS is local translation of axonal mRNAs (Zheng et al., 2001; Smith et al., 2004; Verma et al., 2005; Gumy et al., 2011, 2014; Ji and Jaffrey, 2013; Kar et al., 2017; Sahoo et al., 2018; Terenzio et al., 2018). Protein synthesis at the axonal injury site is required for growth cone formation and is also implicated in activation of a cell body response to injury, triggering regeneration (Verma et al., 2005; Ji and Jaffrey, 2013; Pacheco et al., 2020). Moreover, enhancing translation by dissolving stress granules and thus releasing sequestered mRNAs and translation factors using a dominant negative isoform of G3BP1 increases the extent of regeneration in a sciatic nerve crush model (Sahoo et al., 2018, 2020). Together, these findings suggest a critical role for local translation in enabling axon

* Corresponding author.
*E-mail address:* susanvanerp@gmail.com (S. van Erp).

https://doi.org/10.1016/j.expneurol.2020.113594
Received 28 September 2020; Received in revised form 7 December 2020; Accepted 17 December 2020
Available online 13 January 2021

regeneration. However, the extent to which deficiencies in this local translation might explain the paucity of axonal regeneration in the CNS remains poorly defined.

We have shown previously that a loss of the ability to regenerate occurs as hESC-derived CNS neurons mature in vitro (Koseki et al., 2017), so providing a model system to study the relationship between local translation and regeneration in CNS axons. Here therefore we address the hypothesis that the maturation-related loss of axon regeneration potential in human ESC-derived neurons results from a reduced ability to activate local translation at sites of axotomy, using a combination of cell culture manipulations and proteomics. To do this, we start by confirming the necessity of translation for regeneration in these hESC-derived human neurons. We then show, in support of the hypothesis, that i) local translation occurs in human CNS axons, ii) that increasing regeneration is associated with enhanced local translation and the generation of components of the protein synthesis machinery, and iii) that the decreased regeneration in mature axons is associated with decreased local translation and a fall in expression and function of the components of the protein synthesis machinery. Our work highlights the value of a hESC culture model for studies of CNS axon regeneration and adds significantly to the evidence for an important role of local translation in determining intrinsic regenerative capacity.

## 2. Materials & methods

### 2.1. Cell culture and differentiation of hESC-derived neurons

RC17 hESC cells (Roslin Cells, Scottish Centre for Regenerative Medicine, Edinburgh) were cultured in Essential 8 medium, supplemented with 2 mM L-Glutamine and 0.2% Penicillin Streptomycin (P/S, Gibco, Life Technologies) on Geltrex coated plates (150 μg/ml, Invitrogen) and passaged using EDTA (0.5 mM, Sigma-Aldrich) and used for differentiation towards neural cells of a telencephalic fate (Kirkeby et al., 2012). On day (d)0, stem cells were detached and re-plated to a non-treated dish containing 14 ml neural induction medium (NIM: DMEM/F12: Neurobasal (50% + 50%), 1 x N2, 1× B27, 2 mM L-Glutamine, 0.2% P/S, 10 μM Y-27632, 10 μM SB431542 (SB, R&D systems), 100 ng/ml noggin, 200 ng/ml C24II sonic hedgehog (shh, R&D systems) and 0.9 μM CHIR99021 (CH, Tocris Bioscience) and cultured on a rotating platform to allow embryonic body (EB) formation. On d4, the EBs were plated in neural proliferation medium (NPM: DMEM/F12: Neurobasal (50% + 50%), 0.5 x N2, 0.5 x B27, 2 mM L-Glutamine, 0.2% pen/strep, SB (10 μM), noggin (100 ng/ml), shh, CH) on Poly-ornithine (PO)(1:10000)/Laminin (lam)(5.2 μg/mL)/Fibronectin (FN) (4.35 μg/mL) coated well plates. On d7, the medium was replaced with fresh NPM medium, followed by plain NPM medium on d9. Next, on d11, the cells were replated. Firstly, the cells were washed twice with PBS and a minimal amount of accutase was added for 10 min to allow detachment of the cells. The cells were dissociated from the well plate using a pipette and spun down for 4 min at 0.3 rcf. The cells were resuspended to a density of 10.000 cells/μl in neural differentiation medium NDM (Neurobasal, 1 x B27 (1:50), 2 mM L-Glutamine, 0.2% pen/strep) and added in 7.5 μl droplets to dry PO/FN/lam coated μ-slide 8 well plates (iBidi) and 10 μl droplets to 13 mm PO/FN/lam coated cover glasses or 6-well plates. Cells were kept in the incubator for 10 min to allow attachment of the cells. Next, NDM medium + BDNF (20 ng/ml) + GDNF (10 ng/ml) + AA (0.2 mM) was added to the wells. After 14 days, neuroprogenitor cells are created and medium was changed to NDM medium + BDNF (20 ng/ml) + GDNF (10 ng/ml) + ascorbid acid (0.2 mM) + db-cAMP (500 μM) + DAPT (1 μM) to induce terminal differentiation and maintained until the end of the experiment with the medium changed twice weekly.

### 2.2. Laser-mediated axotomy

Laser axotomy of hESC-derived neurons was performed as described previously (Koseki et al., 2017; Nieuwenhuis et al., 2020). Neurons were axotomised between d40-d65 as stated in text. Except for co-culture with hOPC where transfection took place 10 days prior, neurons were transfected 2–3 days prior to axotomy, with eGFP containing plasmid using lipofectamine 2000 (Invitrogen). The GFP signal was used to visualise single cells within the dense culture and to identify the axon. Only clearly polarised neurons with many dendrites and a single axon were used in the experiments. Axons were severed in vitro using a 365 nm laser (Micropoint, Andor) connected to an Andor spinning disk confocal microscope at >500 μm distal from the cell body on a section of axon free from branches. A single axon cut was made per neuron. Images (z-stack spanning 40 μm) after axotomy were acquired every 20 min for 16 h. Regeneration was classed as the development of a new growth cone followed by axon extension for a minimum of 50 μm.

For analysis of age-related decline in regeneration, we pooled data from previously published experiments (Koseki, 2017; Nieuwenhuis, 2020) and added six additional datapoints from new experiments. A minimum of 10 cells was measured for each datapoint. Each hESC-neuronal conversion was used for two datapoints corresponding to a younger (<d50, typically around d45) and an aged (>d50, typically around d65) time point. This corrects for any potential differences between neuronal culture conversions.

### 2.3. In vitro differentiation and co-culture of hESC-derived OPC

A membrane bound GFP hESC line of RC17s was generated using zinc-finger recombinase. First, the palmitoylation sequence of GAP43 was used to tag GFP. This 60 bp sequence from the N-terminal of GAP43 is associated with its attachment to the membrane (see Supplemental Material 1&2 for plasmid map and sequence). The membrane-targeting GFP was then inserted at the AAVS1 locus. This was done using the pZDonor-AAVS1 Puromycin Vector Kit (Sigma) in conjunction with the CompoZr Targeted Integration Kit (Sigma) as per the manufacturer's instructions. GFP+ hESCs were cultured in StemMACS™ iPS-Brew XF, human medium (Miltenyi Biotec Inc.) on human recombinant laminin-521 coated plates (5 μg/ml, Biolamina) with puromycin (0.25 μg/ml Sigma). Cells were passaged using EDTA (0.5 mM, Sigma). hESCs were differentiated to oligodendroglia as described (Livesey et al., 2016). Briefly, once confluent, colonies were lifted using dispase (1 mg/ml Life Technologies) and collagenase (2 mg/ml,Life Technologies). Embryo bodies were cultured, on a rotatory shaker, in chemically defined medium composed of 50% Iscove's modified Dulbecco's medium (Invitrogen) 50% F12 (Invitrogen), BSA (5 mg/ml, Sigma), 1% chemically defined Lipid 100 (Invitrogen), monothioglycerol (450 μM, Sigma), insulin (7 mg/ml, Roche), transferrin (15 mg/ml, Roche), 1% Antibiotic Antimycotic Solution (Sigma). Embryoid bodies were neuralized with dual-SMAD inhibition (Chambers et al., 2009) by supplementing medium with *N*-acetyl cysteine (1 mM, Sigma), activin inhibitor SB 431542 (10 μM, Sigma), and dorsomorphin (2 μM, Merck Millipore) for 7 days. Neural spheres were caudalized for 7 days in chemically defined medium supplemented with heparin (5 μg/ml, Sigma), *N*-acetyl cysteine (1 mM, Sigma), retinoic acid (0.1 μM, Sigma) and basic fibroblast growth factor (FGF-2) (10 ng/ml, PeproTech). Neural conversion was assessed by the morphology of cells when plated on laminin-coated plates (10 μg/ml, L2020, Sigma). Neuralized spheres were picked and transferred to advanced DMEM (Invitrogen), containing 1% Antibiotic Antimycotic Solution, 1% B27 (Invitrogen), 1% N2 (Invitrogen), 0.5% GlutaMAX (Invitrogen) and heparin (5 μg/ml). Neural spheres were ventralized by supplementing the media with FGF-2 (10 ng/ml, PeproTech), purmorphamine (1 μM, Calbiochem) and retinoic acid (1 μM) for 7 days. FGF2 was then withdrawn from this media for 2 weeks. Oligodendrocyte precursor proliferation was promoted by supplementing the media with FGF2 (10 ng/ml), PDGFα (20 ng/ml, PeproTech), purmorphamine (1 μM), and SAG (1 μM, Calbiochem), IGF-1 (10 ng/ml, PeproTech) and T3 (60 ng/ml, Sigma). Spheres were dissociated after 2 weeks using the Worthington papain dissociation system as per the manufacturer's

instructions and 30,000 cells were added to the neuron cultures.

### 2.4. Visualization and identification of newly-synthesized proteins

#### 2.4.1. OPP tagging and fluorescent labelling for visualization

Neurons were labelled in μ-slide 8 well plates (ibiTreat surface Ibidi). First, the cells were pre-incubated for 30 min with NDM (neurobasal medium containing BDNF, GDNF and ascorbic acid) or NDM supplemented with protein synthesis inhibitors Anisomycin (100 μM) or cycloheximide (CHX) (40 μM) or with cell permeable G3BP1 190–208 peptide (Sahoo et al., 2018). Next, the cells were incubated for 20 min with neurobasal medium containing the Click-iT OPP (20 μM) including the Anisomycin or CHX or medium only in the control group. CHX and OPP bind to the same site, so both Anisomycin and CHX were used to confirm that any reduction in OPP binding was due to a decrease in protein synthesis and not competition for a shared binding site. The cells were washed with PBS and fixed for 15 min at room temperature using 3.7% formaldehyde in PBS. Afterwards, 0.5% TritonX-100 in PBS was added for 15 min to allow permeabilization of the cells. Next, the OPP tagged proteins were fluorescently labelled for visualization. The Click-iT Plus OPP Alexa Fluor 647 reaction cocktail was prepared according to manufacturer's protocol (Thermo Fisher). The cells were washed twice with PBS and incubated with the OPP cocktail for 30 min, protected from light. The cells were rinsed using the Click-iT Reaction Rinse Buffer and incubated for 30 min with HCS NuclearMaskTM Blue Stain solution (1:2000 in PBS). Finally, the cells were washed twice with PBS and ready for immuno labelling.

#### 2.4.2. OPP tagging and biotin labelling for identification using mass spectometry

For biochemistry experiments, cell culture was scaled up to 6-well plates (with 100.000 cells per well) where maximum axonal outgrowth is achieved and mechanic dissection of cell body fraction from axonal fraction is possible. To identify proteins that are translated as a result of axonal injury, cultures were split in injury and control conditions. In the injury group, axons were severed at the proximal end using a scalpel under dissection microscope and returned to the incubator for two hours. To label protein synthesis, cells were incubated with OPP (O-propargyl-puromycin, alkyne analog of puromycin, 20 μM, Sigma) in NDM for two hours. Cells were then washed in ice cold PBS followed by stereotactic dissection to separately collect cell body clusters and remaining isolated axons. Axon and cell body fractions from 3 × 6 well plates were pooled to obtain sufficient cellular fraction material for downstream application. The samples were centrifuged for 10 min at 9000 rcf at 4 °C. The pellet was washed with 1× PBS and centrifuged again for 10 min at 9000 rcf at 4 °C. Pellets were snap-frozen and stored at −80 °C for further analysis. The pellets were lysed using RIPA buffer with protease inhibitor cocktail. The lysate was pre-cleared prior to biotin labelling by incubating with high capacity streptavidin agarose beads. Biotin labelling was done using the Click-iT™ Protein Reaction Buffer Kit (Thermo Fisher) according to the manufacturer's protocol. Cell lysates were incubated with biotin-azide (40 μM, Thermo Fisher) added to the reaction buffer, to enable the binding reaction to alkyne OPP present on newly synthesized proteins. OPP-biotin double-labelled proteins were precipitated, and the dried pellets were stored at −20 °C and shipped on dry ice for further processing. Upon protein clarification, the pulldown and trypsin digest were performed on a Kingfisher duo liquid handling station (Thermo). The lysate was incubated with 5 μl of Streptavidin Dynabeads (Invitrogen) for 4 h at 4 °C under mixing. Following incubation, the beads were washed 2× with 0.3 ml of wash buffer (50 mM Tris-HCl 150 mM NaCl, 1% NP40) and 3× with wash buffer without NP40. The beads were transferred into 100 μl of 2 M Urea, 50 mM TrisCl pH 8, 0.5 μg porcine Trypsin (Promega) and Trypsin and processed as previously described (Turriziani et al., 2014). Mass spectrometry was done using a Lumos Fusion (Thermo) mass spectrometer coupled to an RLS-nano uHPLC (Thermo). Peptides were separated by a 40-min linear gradient from 5 to 30% Acetonitrile, 0.05% Acetic acid separated on an Aurora column (Ionoptiks, Australia). The mass spectrometer was operated using the following setting: MS was set 120 k resolution in the Orbitrap, ions selected for fragmentation were isolated with a window of 1.1 Th, fragmented in the HCD trap with a normalized collision energy of 30 and read out in the ion trap using rapid scanning. Proteins were identified and quantified the MaxQuant software suite using label-free quantification and searching against the human Uniprot database.

### 2.5. Immunocytochemistry

Cells were fixed for 15 min at room temperature using 3.7% formaldehyde in PBS. Where protein synthesis labelling was performed, cells were first processed as described above and immunolabeling was performed on labelled cells. Following fixation or protein labelling, the cells were washed 3 times at room temperature. The cells were blocked by 2% normal donkey serum (NDS), 2% normal goat serum (NGS) and 0.2% triton-x for 30 min. Next, the primary antibody solution was added diluted in blocking buffer (see table). The cells were incubated overnight in the fridge. The next day, the cells were washed 3 times with PBS. The secondary antibody solution, consisting of blocking buffer, donkey/goat anti mouse 488 (Invitrogen, 1:500) and goat anti chicken 568 (Invitrogen, 1:500), was added for 30 min at room temperature. The cells were washed and embedded in Fluoromount-G, followed by microscopic imaging or storage in fridge protected from light. Images were collected using a Leica TCS SP8 confocal microscope with 63× objective and 405, 488 (argon), 552 & 638 nm lasers.

### 2.6. Microfluidic chambers

Coverslips were acid washed in 1 N HCl overnight at room temperature (rotating), rinsed several times with sterile $H_2O$ and stored in 70% ethanol. Prior to use, the coverslips were washed with MQ water, air-dried, and coated overnight with polyornithine (0.01%, Sigma) in 37 °C incubator. The coated cover slips were washed with sterile $H_2O$ and air-dried. Microfluidic chambers with 450 μm grooves (RD450, Xona) were washed with 70% ethanol followed by sterile $H_2O$. Non-plasma bonding was used to mount the chambers to the coated coverslips. Mounted devices were coated overnight with laminin (0.6 mg/ml) and fibronectin (0.5 mg/ml). Cell suspensions (50,000 cells) of d11 neurons (prepared according to described cell culture protocol) were plated in the proximal compartment and cultured in NDM medium.

### 2.7. Image analysis

Fluorescent intensity of antibody staining and OPP labelling was quantified using confocal microscopy images collected as described above. After collection of the confocal z-stacks, the images were exported to FIJI. Output of the axon data was generated by a custom-made macro. Using this macro, a fixed threshold (which was determined for each batch of labelled cells and where each batch contained all experimental conditions and controls) was set to determine the areas positive and negative for axons (SMI312) and newly synthesized proteins (OPP). Cell body containing areas were removed from the images to prevent misidentification of the protein content in the axons due to a much higher amount of protein synthesis in the cell bodies. Next, the overlap between the OPP positive areas and SMI positive areas was determined for each frame in the z-stack and divided by the axonal area to correct for differences in axon density in the different frames. The means of these areas (overlap/area axons per frame) were compared between the different experimental conditions and controls. Similarly, the level of newly synthesized proteins in the cell bodies was determined by measuring the mean OPP intensity of the z-stack within the Hoechst-stained area. This avoids variability due to irregular cell body shapes. Significant differences between the two groups (d45 and d65) were

tested using an independent *t*-test.

### 2.8. Western blot

Cell pellets were lysed in 50 μl lysis buffer (RIPA buffer; Thermo Scientific, supplemented with protease inhibitor cocktail; Calbiochem). Concentration was measured with the Pierce BCA kit (ThermoFisher) and the Omega FluoSTAR microplate reader (BMG LabTech). For western blot analysis, 7.5 μg protein was used per slot. Cell lysates were denatured in 1× NuPage LDS Sample Buffer buffer (Novex, Life Technologies) supplemented with 1:10 β-mercapto-ethanol (Sigma-Aldrich) followed by incubation for 5 min at 95 °C. Next, the cell lysates were separated on a gradient BioRad gel (7–12%) in 1× Tris Glycine SDS (TGS) running buffer (BioRad). Proteins were transferred to Immobilon-P membrane (Millipore) in transfer buffer (1× NuPage transfer buffer (Novex, Life Technologies), 10% ethanol) at 160 mA for 1 h. Following a washing step in Tris-buffered Saline with 0.01% Tween-20 (TBS-T, Sigma- Aldrich), blots were blocked in 5% non-fat milk powder (Tesco) in TBS-T for 30 min. Subsequently, blots were incubated overnight (O/N) with primary antibody *(see Table in Material and Methods)* in TBS-T at 4 °C. The next day, the blots were washed in TBS-T and incubated with HRP-conjugated secondary antibodies anti-mouse (1:60,000, Jackson ImmunoResearch) or anti-rabbit (1:30,000, Thermo Scientific) for 1 h at RT. The sections were washed in TBS-T and antibody binding was visualized using ECL kit (Thermo Fisher) and a medical film processor (Konica Minolta Medical & Graphic). Films were digitised and then analysed with ImageJ Software. Background was subtracted and β-Actin bands were used as loading control.

Material and methods; primary antibodies

| Antibody name | Manufacturer | Number | Species |
|---|---|---|---|
| Purified Map2 (PCK-554P) | BioLegend | 822,501 | Chicken |
| Neurofilament marker, pan-axonal | Biolegend | SMI-312R | Mouse |
| B3-Tubulin | Abcam | ab7751 | Mouse |
| Tyrosine Hydroxylase (TH) | EMD Millipore | AB152 | Rabbit |
| Sortilin | Abcam | ab16640 | Rabbit |
| EIF3b | Atlas Antibodies | HPA048983 | Rabbit |
| Fibronectin (*H*−300) | Santa Cruz | sc-9068 | Rabbit |
| Map2 (AP-20) | Abcam | ab11268 | Mouse |
| RPL35 | Abcam | ab190162 | Rabbit |
| RPL26 | Bethyl Laboratories | A300-686A-M | Rabbit |
| rRNA Y10b | Santa Cruz | sc-33,678 | Mouse |
| b-Actin | Merck Millipore | MAB1501 | Mouse |
| HuR | Merck Millipore | 07–468 | Rabbit |
| FMRP | Cell Signaling | 4317 s | Rabbit |
| Olig2 | Atlas Antibodies | HPA003254 | Rabbit |

### 2.9. Mass spectrometry of axonal proteins at d45 and d65 in vitro

To compare the proteomes of axons grown by human ES cell-derived neurons after 45 and 65 days in vitro cultures in 6-well plates were used, enabling 100.000 cells to be plated into the centre of each well so as to allow radial axonal outgrowth towards the edge of the well. For sample collection, the wells were washed twice with cold phosphate-buffered saline (1× PBS, Life Technologies). Subsequently, 500 μl PBS was added. The cell bodies, forming a pellet in the middle of the well, were removed and collected using a dissection microscope (Olympos) and scalpel. Next, the remaining axons were collected in PBS by gently pipetting. Axons from 3 × 6-well plates were pooled to obtain sufficient material for proteomic analysis. The samples were centrifuged for 10 min at 9000 rcf at 4 °C. The pellet was washed with 1× PBS and centrifuged again for 10 min at 9000 rcf at 4 °C. Pellets were snap-frozen and stored at −80 °C for further analysis.

For liquid chromatography-tandem mass spectrometry (LC-MS/MS), frozen cell and axon pellets were lysed in 50 μl lysis buffer (RIPA; Thermo Scientific +1:100 protease inhibitors) and protein concentration was measured. For each sample 50 μg of protein was used for LC-MS/MS. Proteins in urea sample buffer were loaded on a pulse gel for 5 min. The proteins were digested on gel O/N with trypsin. Once digested, the peptides were separated using reversed phase chromatography. Next, the samples were run in the Thermo Scientific QExactive Mass Spectrometer (Michalski et al., 2011). The peptides were identified with a human uniport database and MASCOTT. For quantification, Progenesis software was used. Proteins with less than 2 unique peptides were excluded from further analysis. Functional classification by gene ontology (GO) was performed in PANTHER, as described in (Mi et al., 2013). Enriched biological processes were identified by comparing to the whole human genome PANTHER database.

## 3. Results

### 3.1. Protein translation is required for regeneration of the axons of human ES cell derived neurons

In order to examine the requirement for protein translation in axonal regeneration by human CNS neurons, we used our previously described protocol to generate neurons from human ES cells (Koseki et al., 2017; Nieuwenhuis et al., 2020). These neurons, the majority of which are dopaminergic, extend long axons (>1 mm) in cell culture. These were cut using laser-mediated axotomy to specifically target individual axons, after which we followed their response overnight (Fig. 1A,B). When cut at <d50, the majority of the severed axons regenerate with the formation of a new growth cone at the proximal end of the cut site. This regenerative capacity declines as neurons age in culture and by d65 has reduced significantly, as we have shown previously (Hiroaki Koseki et al., 2017; Nieuwenhuis et al., 2020). However, when we treated young <d50 (ranging from d42-45) hESC-derived neuronal cultures with cycloheximide (CHX) to block protein synthesis and performed in vitro axotomy, no new growth cone formation was seen and no axonal regeneration takes place (Fig. 1C). Importantly, motility of the growth cones at the ends of unsevered axons was not impaired by CHX, and cell survival and cell body motility of the neurons with severed axons were also unaffected by CHX (1D and Supplemental Videos). Together these results show that protein translation is required for formation and motility of new growth cones and axon regeneration, but not for motility of pre-existing growth cones on intact axons, confirming the specificity of the effect of protein synthesis inhibition on regeneration.

### 3.2. Local translation occurs in the axons of human ES cell-derived neurons

The translation required for regeneration as identified by the CHX experiments above could occur in either or both the cell body and axonal compartments. To test for the presence of local translation in the axonal compartment, we used O-Propargyl Puromycin (OPP) to tag newly synthesized peptides and Click chemistry to fluorescently label OPP in the cell body and axon compartments (Sahoo et al., 2018). These experiments clearly showed OPP-labelled proteins in the axons of the human ESC-derived neurons, at distances of >200 μm from the cell body and after 20 min labelling time, arguing for the presence of local translation (Fig. 2A). Moreover, the presence of OPP-labeling in axons and cell bodies is reduced by treatment with translation inhibitors cycloheximide (CHX) and anisomycin (ANI) (Fig. 2A) applied at the time of axotomy. Next, we combined OPP labelling with immunostaining for components of translation machinery including translation initiation factor Eif3B, ribosomal protein RPL26 and rRNA (Fig. 2B,C and Suppl Figs. S1 and S2). The presence of these translation-related proteins alongside OPP-labelled newly synthesized peptides in axons further confirms the presence of local translation. Nevertheless, the use of OPP tagging to identify newly-synthesized proteins in this way does not

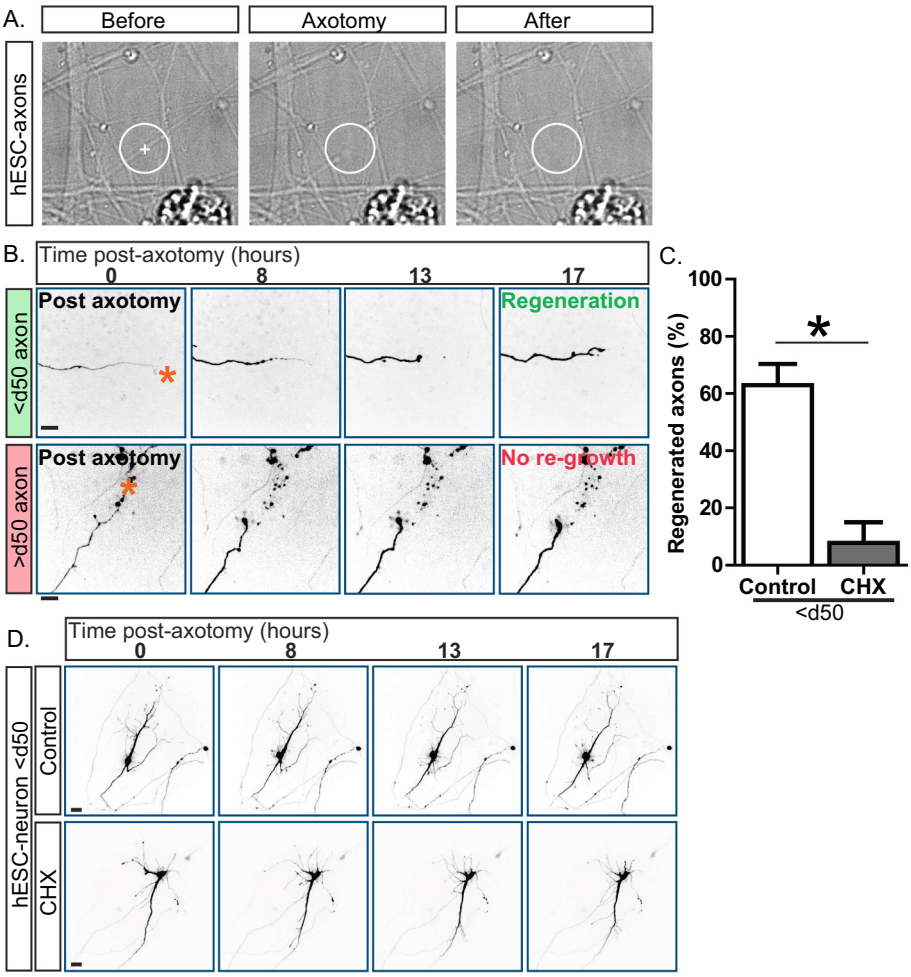


**Fig. 1.** Axon regeneration of hESC-derived neurons declines with age and requires protein synthesis. **A**. Bright-field images of targeted axon before, during and after laser-mediated axotomy of d31 hESC-derived neuronal culture. Scale bar 20 μm. **B**. Examples of regeneration (top) or not (bottom). GFP-transfected neurons were axotomized and imaged over 17 h. After initial retraction, a growth cone forms and regeneration starts, or an immobile stump forms with no regrowth. Scale bar 20 μm. **C**. Blocking protein synthesis with cycloheximide (CHX) prevents axon regeneration in young (d42-45) hESC-derived neurons. $N = 3$ experiments, with >20 axons per experiment. $^*P = 0.0074$ unpaired *t*-test Welch correction. **D**. Examples of <d50 (exact age of both cells in image is d45) neuronal cell bodies from the experiment in C that were treated as control or with CHX overnight. Image sequence shows cell body motility and dendritic outgrowth in both conditions. Scale bar 20 μm.

distinguish whether these proteins are indeed locally synthesized in the axon or synthesized in the soma and then transported to the axon.

To address this issue, we performed two sets of experiments. First, to confirm sustained levels of local protein synthesis we acutely separated axons from cell bodies (age < d50) using a scalpel as shown in Fig. 2D,E, followed by OPP incubation. In the 20 min time window following cell body separation, local axonal protein synthesis took place at the same rate as in the axons of intact neurons, as measured by the level of OPP fluorescent labelling on either side of the cut once the culture was fixed and stained (Fig. 2F). Second, to exclude the possibility that changes in the transport rate from the cell bodies contributes significantly to the OPP-tagged proteins observed, we cultured hESC-derived neurons in microfluidic chambers. Here, cell bodies are restricted to one compartment and axons extend into a second compartment. The axons in this culture grew through the microgrooves separating the two compartments, as shown in Fig. 2G,H. OPP was then added to the cell body compartment (at age < d50) and the axonal intensity of newly synthesized proteins was compared in axons from either the cell body or the axonal compartment. The almost complete absence of OPP labelling in the axonal compartment 20 min following its addition to the cell body compartment (Fig. 2I) clearly indicates that there is a minimal contribution of OPP-tagged newly synthesized proteins from the cell body to any observed changes in OPP labelling in the axon. We conclude, therefore, that local translation occurs in the axons of in vitro cultured hESC-derived neurons.

### *3.3. Increased regeneration of human ES cell -derived neurons is associated with increased local translation within the axons*

Next, we asked whether increased regeneration is associated with increased local translation in the axons. To increase regeneration, we use a co-culture system where hESC-derived neurons are cultured in the presence or absence of hESC-derived oligodendrocyte precursor cells (OPC). We reasoned that OPC would enhance axon regeneration in vitro, given they are known to promote neurite outgrowth in vitro and improve functional regeneration in vivo (Keirstead et al., 2005; Sharp et al., 2010; Haas and Fischer, 2013; Hayakawa et al., 2015; Hayakawa et al., 2016; Jin et al., 2018). We used RC17 hESC cells that were genetically targeted to constitutively express GFP and differentiated them into glial precursors. Non-fluorescent hESC were differentiated into neurons and transfected using lipofectamine with an mCherry expression vector, after which the GFP+ glial precursors were plated together with the transfected d45 neurons. This allows us to distinguish the two cell populations in live cell imaging experiments.

Our in vitro axotomy assay was performed after ten days of co-culture to allow for both further differentiation of the glial precursors into OPC and simultaneous aging of the neuronal population from d45 to d55. The presence of OPC did, as predicted, increase the percentage of regenerating axons from 14% (±2.3% SD) in control experiments to 45% (±1.5% SD) (Fig. 3A). This is a meaningful increase for these aged (>d50) cultures where we typically see regeneration of less than 30% of the axons. Next, we asked whether the increased regeneration potential in neurons co-cultured with hOPC could be associated with increased axonal protein synthesis. We used the OPP assay described above to

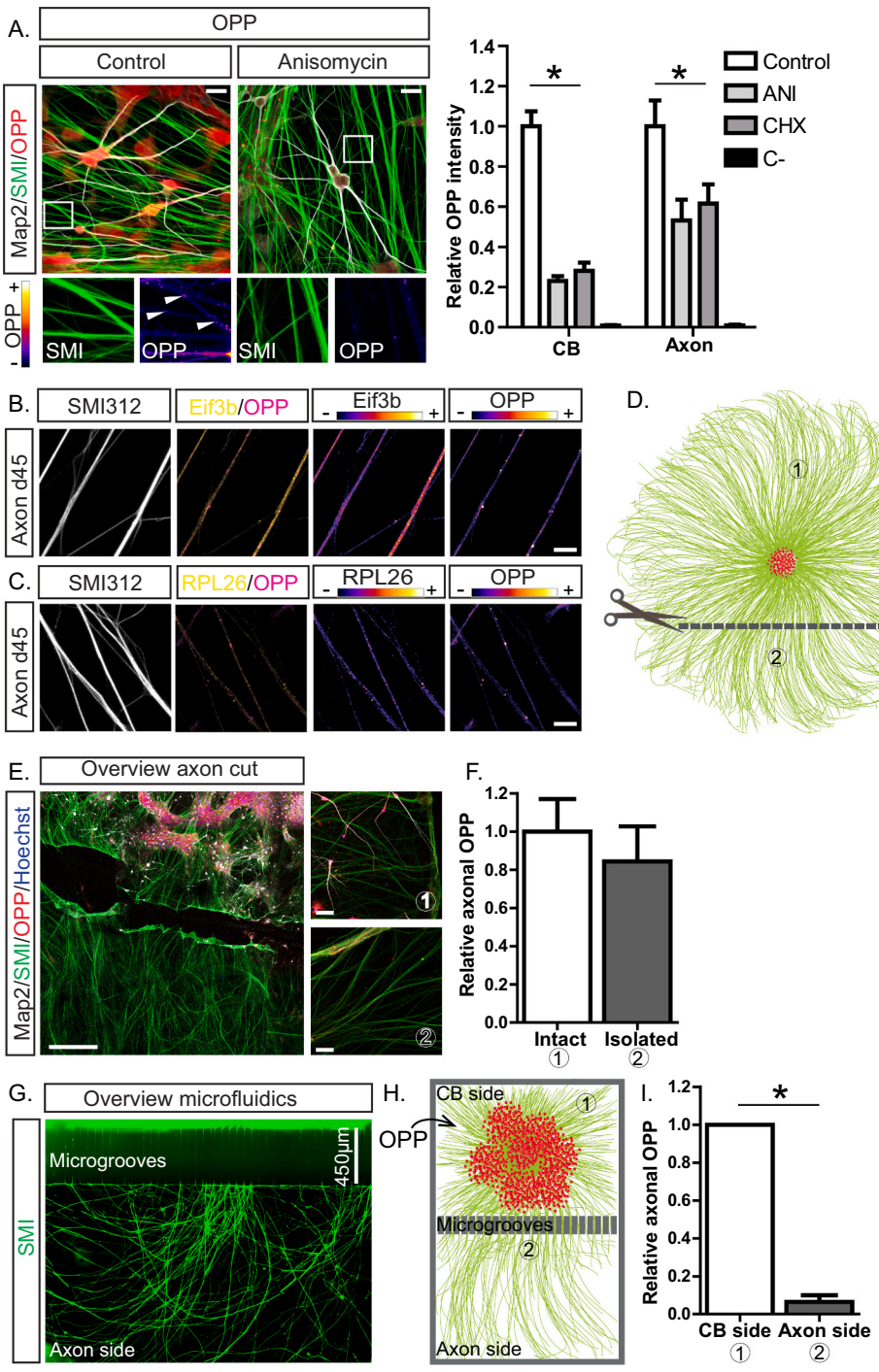


**Fig. 2.** Local axonal protein synthesis takes place in the axons of hESC-derived neurons. **A.** OPP-labelling (red) is present in axons (SMI312, green) and cell bodies (Map2, white) and translation inhibitor Anisomycin (ANI) reduces OPP incorporation in both (scale bar 20 µm). Magnification shows punctate presence (arrow heads) of OPP (range indicator) in axons (SMI312, green). Right panel shows quantification of OPP labelling in cell bodies (CB) and axons of hESC-derived neurons. Treatment with OPP alone (control) was used to normalise the conditions with OPP and cycloheximide (CHX) or ANI. In the negative control condition (C-) no OPP was present, showing the level of non-specific staining. $N = 5$ experiments, 6–10 images per condition per experiment. $^*P < 0.001$ 2-way ANOVA. **B—C.** OPP labelling co-localises with translation initiation factor Eif3B (B) and ribosomal protein RPL26 (C) in axons (SMI312, left panel). Overlay image with OPP and Eif3B or RPL26 is shown as well as the individual images to illustrate the distribution of protein and protein synthesis in the axons. Scale bar 10 µm. **D.** Schematic overview of experimental setup to test whether axonal peptides are locally synthesized or transported from the cell body. Axons were cut on one side of the culture and OPP was added. OPP-labelling was measured in axons from location 1 (intact) and location 2 (separated from cell body). **E.** Overview image of neuronal culture on cut-side (location 2) with close up examples of axons in location 1 and location 2 on right side (overview image scale bar 700 µm, close up scale bar 50 µm). Map2 is white, SMI312 is green, OPP is red and nuclei (Hoechst) are blue. **F.** Quantification of OPP intensity in axons normalized to average level in intact axons. $N = 3$ experiments, 6–10 images per condition per experiment. $P = 0.5772$ unpaired $t$-test Welch correction. **G.** Overview of hESC-derived neuronal culture in microfluidics chamber. The cells are plated on the opposite side of microgrooves and axons can extend into the axonal compartment (axon side). Axons were immunolabeled with SMI312 (green). **H.** Schematic overview of the experimental setup to assess the contribution of transport from newly synthesized proteins from the cell body to the axon using microfluidics chamber. OPP is added to the cell body compartment and axonal levels of OPP are measured in both compartments after 20 min (location 1 and 2). **I.** Quantification of experiment in G. The level of OPP in axons on the cell body side was used for normalization. N = 3 experiments, 6–10 images per condition per experiments. $^*p = 0.0004$ paired t-test.

demonstrate local axonal translation in the cells used in the axotomy assay. Immunolabeling with OPC marker transcription factor Olig2 and axonal marker SMI312 allowed us to analyse the level of translation in axons cultured in proximity to hOPC and axons cultured under control condition (Fig. 3B). The level of axonal OPP labelling was significantly increased in co-culture conditions, indicating that axonal regeneration is associated with increased axonal protein synthesis.

### *3.4. Regeneration-associated proteins generated by local axonal translation include those involved in protein synthesis*

The OPP technology also enabled us to address the identity of the axonally-synthesized proteins generated during the regenerative process, making use of a modified OPP labelling protocol to tag newly synthesized proteins with biotin. The biotin-tagged peptides were then

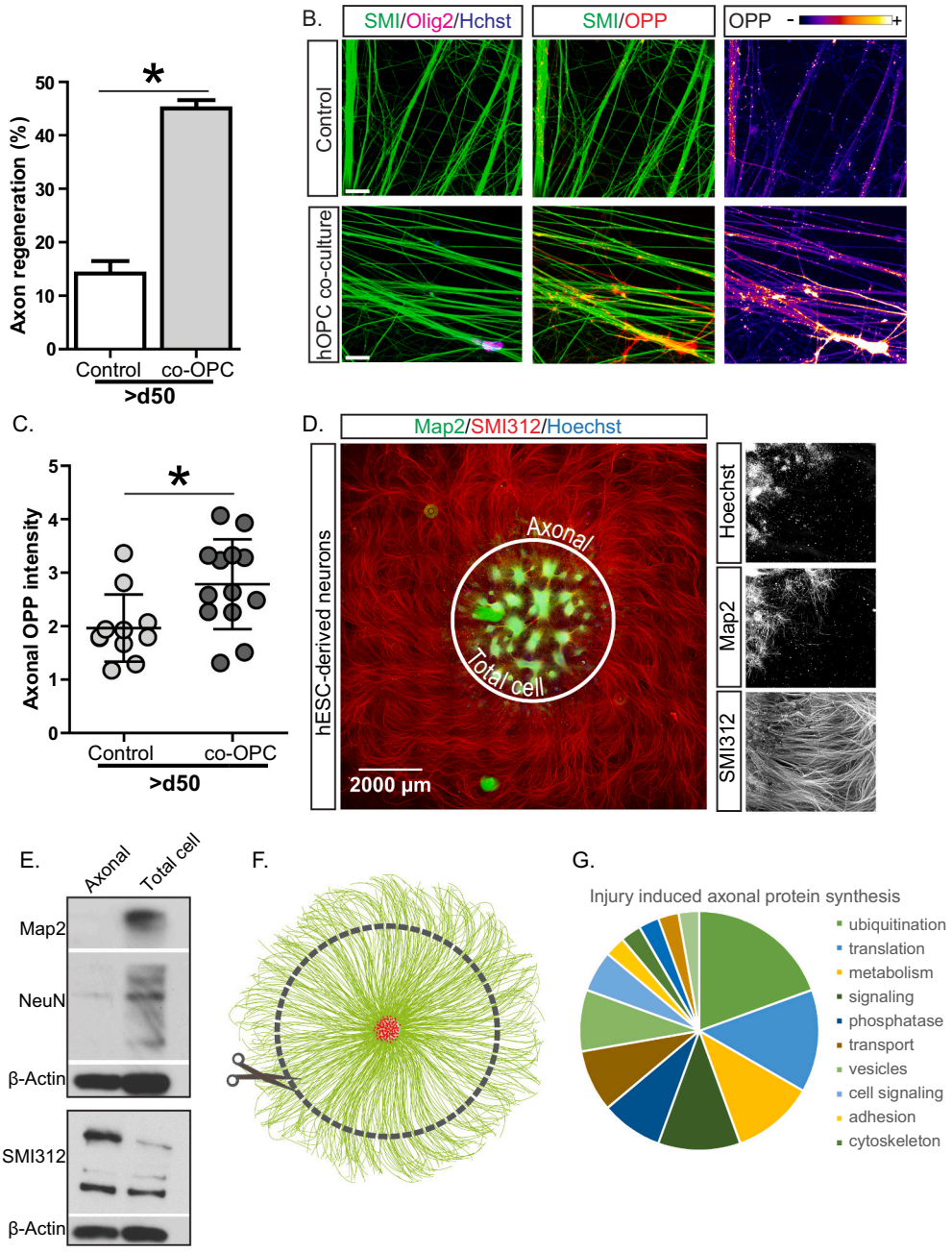


**Fig. 3.** Axonal regeneration is associated with increased axonal protein synthesis and an increase in protein synthesis machinery. **A.** Co-culture of >d50 hESC-derived neurons with hESC-derived OPC increases the percentage of regenerating axons following laser-mediated axotomy. To calculate regeneration, images (z-stack spanning 40 µm) after axotomy were acquired every 20 min for 16 h. Regeneration was classed as the development of a new growth cone followed by axon extension for a minimum of 50 µm. $N = 2$ experiments, >10 cells per experiment. $P = 0.04$ unpaired t-test Welch correction. **B.** Axonal translation (OPP) was measured under control conditions or in co-culture with hOPC. In the presence of hOPC (Olig2+ cell in bottom panels, showing a field of view from the un-injured area of an axotomy experiment) a higher level of OPP is seen in axons (SMI312, green). Scale bar 20 µm. **C.** Quantification of B. OPP intensity in axons was measured. $N = 13$ images from 2 experiments. $P = 0.0239$ Mann-Whitney $U$ test. **D.** Typical morphology of hESC-derived neuronal culture with a central cluster containing cell bodies (nuclei, Hoechst, blue) and dendrites (Map2, green) and radially extending axons (SMI312, red). Total cell fraction contains cell bodies and axons and can be separated from the axonal fraction containing axons only. **E.** Western blot analysis confirms the absence of dendritic and nuclear proteins from the axonal fraction compared to total cell fraction. Axonal marker SMI312 is enriched in the axonal fraction. **F.** Schematic overview of experimental setup to assess axonal injury-induced protein synthesis. Axons of d45 hESC-derived neurons were axotomized using scalpel prior to OPP labelling and compared to control uninjured condition to identify changes in protein synthesis. **G.** Newly synthesized proteins were labelled with OPP and tagged with biotin. Biotin pull down followed by mass spectrometry resulted in a snapshot of the injury-response translatome. The pie chart shows protein categories that were enriched after injury.

purified with streptavidin beads and analysed using mass spectrometry (Sup Fig. S3). To obtain enough material to perform proteomics on severed axons, we took advantage of the morphological properties of maturing dopaminergic neurons derived from hES cells. In the differentiation protocol we used, neural progenitors are plated at d11 to facilitate differentiation. During and after differentiation, the cells extend long axons and show little cell body migration. This results in a culture containing a central cluster of cell bodies from which large numbers of axons grow radially for as much as 6 mm (Fig. 3D). We exploited this property of these cultures to isolate the axons from the cell bodies using a dissection microscope and a scalpel. The collected axonal fraction was used for protein extraction. Testing the ability of the protocol to separate cell body and axonal proteins, we used western blotting and confirmed the absence of dendritic markers (Map2) and nuclear markers (NeuN) in the axonal fraction (Fig. 3E). The axonal fraction was also enriched in axonal marker (SMI312) protein when compared to the total cell fraction (Fig. 3E).

With this method, we were also able to examine locally synthesized peptides in the cell bodies and axons of uninjured d45 neurons and of d45 neurons that had been axotomized using a scalpel. To do this, one group of cell cultures were 'injured' by severing the axons with a scalpel (as shown schematically in Fig. 3F) while the control group were left intact. Two hours after the injury all cultures were incubated with OPP for a further two hours (the average time growth cone formation is usually seen in our setup is 4 h after injury) and the axons and corresponding cell bodies were collected separately for protein extraction, biotin labelling, pull down and mass spectrometry. As a response to injury, 36 proteins were synthesized at a higher rate in the axonal fraction and 41 in the total cell fraction (Tables 1 and 2). Among the upregulated proteins in the axons, the largest group is related to ubiquitination and another 20% are associated with protein synthesis, confirming that part of the axonal response to injury is to increase the

**Table 1**
Injury-induced protein synthesis in axons

| Injury-induced protein synthesisis (axons) | | |
|---|---|---|
| Protein names | Gene names | Ratio cut/ uncut |
| Phosphomevalonate kinase | PMVK | 9.73 |
| Creatine kinase M-type | CKM | 8.23 |
| **Proteasome subunit beta type-4** | **PSMB4** | 7.04 |
| Methionine–tRNA ligase, cytoplasmic | MARS | 4.20 |
| Excitatory amino acid transporter 2 | SLC1A2 | 3.49 |
| Vacuolar protein sorting-associated protein 4B | VPS4B | 3.43 |
| E3 ubiquitin-protein ligase HUWE1 | HUWE1 | 3.26 |
| **26S proteasome non-ATPase regulatory subunit 3** | **PSMD3** | 2.91 |
| Insulin-like growth factor 2 mRNA-binding protein 3 | IGF2BP3 | 2.83 |
| 60S ribosomal protein L30 | RPL30 | 2.75 |
| Tyrosine-protein phosphatase non-receptor type 9 | PTPN9 | 2.66 |
| Nuclear mitotic apparatus protein 1 | NUMA1 | 2.51 |
| ATPase ASNA1 | ASNA1 | 2.21 |
| **Microsomal glutathione S-transferase 3** | **MGST3** | 2.12 |
| Ig kappa chain C region | IGKC | 2.01 |
| Cystatin-A;Cystatin-A | CSTA | 1.98 |
| **Plexin-B2** | **PLXNB2** | 1.90 |
| Tubulin alpha-1B chain;Tubulin alpha-4A chain | TUBA1B; TUBA4A | 1.85 |
| 14 kDa phosphohistidine phosphatase | PHPT1 | 1.84 |
| Leucine-rich repeat-containing protein 57 | LRRC57 | 1.75 |
| Guanine nucleotide-binding protein subunit beta-4 | GNB4 | 1.75 |
| Leucine–tRNA ligase, cytoplasmic | LARS | 1.64 |
| IST1 homolog | IST1 | 1.61 |
| **E2/E3 hybrid ubiquitin-protein ligase UBE2O** | **UBE2O** | 1.58 |
| Suppressor of G2 allele of SKP1 homolog | SUGT1 | 1.53 |
| **GMP reductase 2** | **GMPR2** | 1.53 |
| Lysosomal Pro-X carboxypeptidase | PRCP | 1.47 |
| Katanin p60 ATPase-containing subunit A-like 2 | KATNAL2 | 1.46 |
| **E3 ubiquitin-protein ligase RBX1** | **RBX1** | 1.42 |
| Gasdermin-A | GSDMA | 1.41 |
| Arf-GAP domain and FG repeat-containing protein 1 | AGFG1 | 1.39 |
| **AP-3 complex subunit mu-1** | **AP3M1** | 1.34 |
| UPF0160 protein MYG1, mitochondrial | C12orf10 | 1.34 |
| Guanine nucleotide-binding protein G(I)/G(S)/G (T) subunit beta-2 | GNB2 | 1.31 |
| **Gamma-soluble NSF attachment protein** | **NAPG** | 1.29 |
| Astrocytic phosphoprotein PEA-15 | PEA15 | 1.29 |

The axons of in vitro hESC-derived neurons were cut using a scalpel, incubated with OPP and compared to an uninjured control group. Following OPP labelling, proteins were isolated from the axonal fraction and OPP was tagged with biotin (click chemistry). Biotin was pulled down with streptavidin and the newly synthesized protein fraction was analysed using mass spectrometry. The table shows the identified proteins that were upregulated in injured axons >1.25 times compared to uninjured axons. Proteins in bold overlapped with a previous study identifying axonal protein translation (Shigeoka et al., 2016).

synthesis of the machinery required for local translation and regeneration (Fig. 3G and Table 1).

### 3.5. Axonal maturation and loss of regenerative ability is associated with decreased local translation and decreased levels of the components required for protein synthesis

We have previously established the time course over which the loss of the ability to regenerate occurs as hESC-derived neurons mature in vitro (Koseki et al., 2017). Here we first extended and reanalysed this data as described in the methods, showing that an average 70% of neurons up to d45 can regenerate successfully, whereas the percentage of regenerating axons drops to below 30% from d50 to d65 (Fig. 4A). To determine whether this is associated with a decrease in local translation within axons we measured the OPP signal intensity in axons and cell bodies of d45 and d65 neurons. We found that while the level of protein synthesis is unchanged in cell bodies, there is a significantly lower level of newly synthesized proteins in older axons (Fig. 4B).

**Table 2**
Injury-induced protein synthesis in total cells

| Injury-induced protein synthesisis (total cell) | | |
|---|---|---|
| Protein names | Gene names | Ratio cut/ uncut |
| Dual specificity mitogen-activated protein kinase kinase 4 | MAP2K4 | 7.10 |
| Kynurenine–oxoglutarate transaminase 3 | CCBL2 | 4.22 |
| AP-3 complex subunit mu-1 | AP3M1 | 4.17 |
| Methionine–tRNA ligase, cytoplasmic | MARS | 3.65 |
| NADH dehydrogenase 1 beta subcomplex subunit 10 | NDUFB10 | 3.32 |
| ATPase ASNA1 | ASNA1 | 3.01 |
| Plexin-B2 | PLXNB2 | 2.81 |
| Ras-related protein Rab-21 | RAB21 | 2.51 |
| NAD kinase 2, mitochondrial | NADK2 | 2.30 |
| Eukaryotic translation initiation factor 3 subunit G | EIF3G | 2.29 |
| Rho-related GTP-binding protein RhoC | RHOC | 2.28 |
| Rho GTPase-activating protein 35 | ARHGAP35 | 2.23 |
| Myomegalin | PDE4DIP | 2.08 |
| Very long-chain specific acyl-CoA dehydrogenase | ACADVL | 2.07 |
| Disco-interacting protein 2 homolog B | DIP2B | 2.02 |
| MAGUK p55 subfamily member 2 | MPP2 | 2.01 |
| Small ubiquitin-related modifier 1 | SUMO1 | 1.98 |
| E3 ubiquitin-protein ligase NEDD4-like | NEDD4L | 1.97 |
| Protein transport protein Sec23A | SEC23A | 1.96 |
| Eukaryotic translation initiation factor 2 subunit 3 | EIF2S3; EIF2S3L | 1.95 |
| Translin | TSN | 1.93 |
| Ataxin-10 | ATXN10 | 1.77 |
| Cell division cycle 5-like protein | CDC5L | 1.75 |
| Ran GTPase-activating protein 1 | RANGAP1 | 1.71 |
| Hydroxysteroid dehydrogenase-like protein 2 | HSDL2 | 1.69 |
| Arf-GAP domain and FG repeat-containing protein 1 | AGFG1 | 1.66 |
| Low-density lipoprotein receptor-related protein 1 | LRP1 | 1.59 |
| Rho guanine nucleotide exchange factor 2 | ARHGEF2 | 1.59 |
| Cystatin-A;Cystatin-A, N-terminally processed | CSTA | 1.55 |
| Phosphatidylinositol transfer protein alpha isoform | PITPNA | 1.55 |
| Calumenin | CALU | 1.51 |
| Mevalonate kinase | MVK | 1.45 |
| Guanine nucleotide-binding protein subunit beta-2 | GNB2 | 1.45 |
| Striatin-4 | STRN4 | 1.44 |
| Insulin-like growth factor 2 mRNA-binding protein 3 | IGF2BP3 | 1.44 |
| Glutaminase kidney isoform, mitochondrial | GLS | 1.41 |
| Thioredoxin domain-containing protein 5 | TXNDC5 | 1.41 |
| 26S proteasome non-ATPase regulatory subunit 9 | PSMD9 | 1.38 |
| Methylmalonate-semialdehyde dehydrogenase | ALDH6A1 | 1.34 |
| Cytosol aminopeptidase | LAP3 | 1.33 |
| Leucine–tRNA ligase, cytoplasmic | LARS | 1.27 |

The axons of in vitro hESC-derived neurons were cut using a scalpel, incubated with OPP and compared to an uninjured control group. Following OPP labelling, proteins were isolated from the cell body (total cell) fraction and OPP was tagged with biotin (click chemistry). Biotin was pulled down with streptavidin and the newly synthesized protein fraction was analysed using mass spectrometry. The table shows the identified proteins that were upregulated in injured cells >1.25 times compared to uninjured cells.

To determine potential mechanisms for this loss of local translation between d45 and d65 we turned to another proteomics approach, using our cultures where axons growing out radially are separated from the cell bodies prior to protein isolation. Now, we aimed to compare any age-related changes in the axonal proteome and we therefore used mass spectrometry to identify the complete proteome of axons at different ages. We performed mass spectrometry in triplicate (from three separate conversions from hESC to differentiated neurons) at the two time points (d45 and d65). This analysis revealed a switch in the protein phenotype associated with the loss of regenerative ability between d45 and d65. We

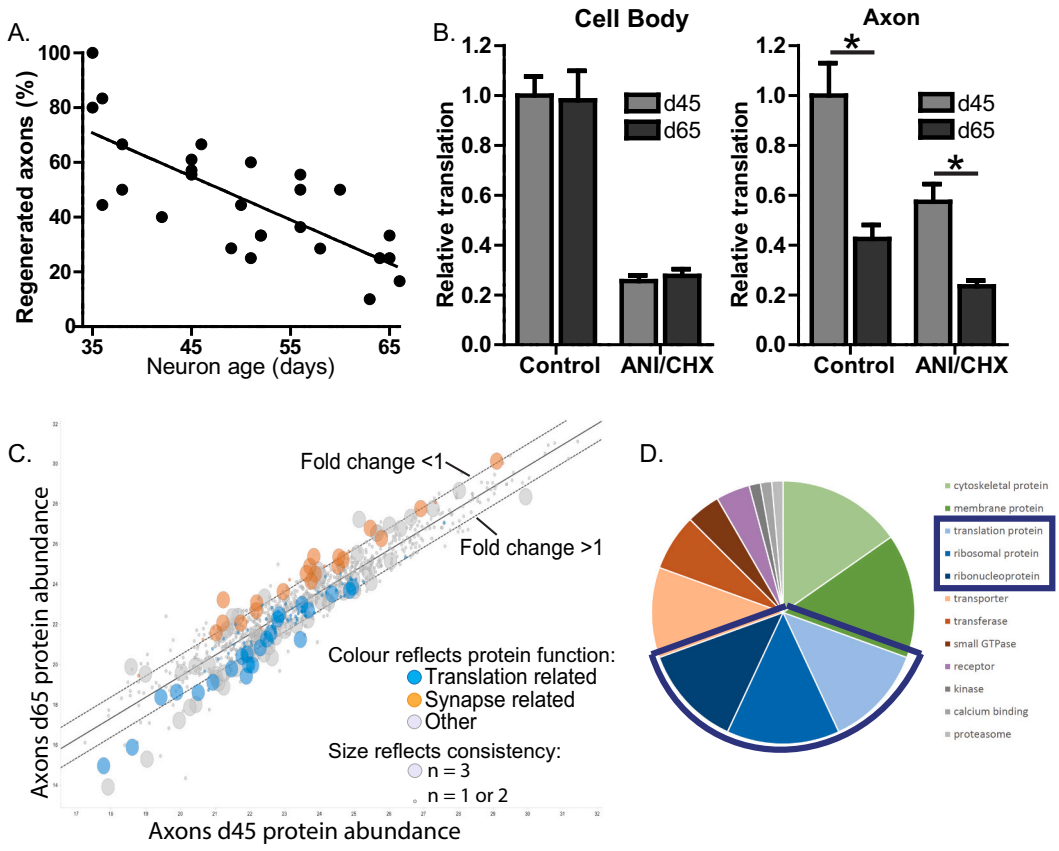


**Fig. 4.** Both axonal regeneration, level of local translation and axonal presence of translation machinery decline with neuronal age.
**A.** The percentage of axons that successfully regenerate following laser-mediated axotomy declines with age in hESC-derived neurons. Linear regression $R^2 = 0.56$, $p < 0.0001$. **B.** Quantification of OPP intensity in cell bodies and axons of d45 and d65 hESC-derived neurons. $N = 5$ (d45) $n = 7$ (d65) experiments with 6–10 images per condition per experiment. $P < 0.001$ 2-way ANOVA. **C.** Comparison of proteomics data from d45 (protein abundance on x-axis) versus d65 (protein abundance on y-axis) axons. Colours indicate protein function, with synapse-related proteins orange, translation-related proteins blue and all other proteins grey. Mass spectrometry was performed in triplicate and dot size is used to indicate the consistency between experiments. Large dots are proteins that were consistently changed ($n = 3$) between d45 and d65, small dots are proteins that were unchanged in one or two experiments ($n = 1$–2). **D.** Pie chart distribution of the functional categories that proteins abundant at d45 compared to d65 belong to.

observed a decrease in the level of translation-related proteins, with a parallel increase in the level of synapse-related proteins and mitochondrial/metabolism processes (Fig. 4C,D, Table 3). For example, we observed decreased levels of the ribosomal protein RPL26 and the translation initiation factor Eif3B. These changes were validated using immunofluorescence, where RPL26 and Eif3B were detected in axons (SMI312 positive) of both d45 and d63-65 hESC-derived neurons. A significant reduction was observed at d63-65 compared to d45 (Fig. S3). By contrast another ribosomal protein RPL35 did not show any changes in level in the immunofluorescent analysis. Illustrating the specificity of these changes to the axonal compartment, we observed the opposite change in Eif3B in the cell body, with an increase in level observed at d65. We conclude, therefore, that the loss of regenerative ability at d65 is associated with a reduction in the presence within axons of the proteins required for local translation.

### *3.6. Decreased local translation and regeneration of mature axons is not reversed by releasing sequestered axonal mRNAs*

To explore the consequences of the observed reduced axonal levels of proteins required for local translation within axons, we examine the effect of increasing axonal mRNAs available for translation. If the level of the axonal proteins required for translation is a limiting factor for local translation and for regeneration, then we would predict that increasing available mRNAs will have no effect on axon regeneration. To do this, we used the previously described cell permeable peptide containing the G3BP1 190–208 domain, which acts as a dominant negative form of G3BP1, competing with the full-length protein as a component of the stress granules that sequester unused mRNAs and releasing the repressed RNA, translation factors and RNA-binding proteins (Sahoo et al., 2018). In primary (young) CNS axons and in the PNS this has been previously shown to result in increased protein synthesis in vitro, with increased axonal regeneration in vivo seen in the PNS (Sahoo et al., 2018). In our experiments using aged (d61-65) hESC-derived neurons, however, no effect of the peptide was seen in the level of protein synthesis, as measured using OPP as above (Fig. 5A,B). We conclude, therefore, that these more mature axons lack the ability to increase local translation of mRNAs released from G3BP1-containing stress granules. In line with this, there was no increase in the percentage of regenerating axons in aged peptide-treated axons compared to control axons (Fig. 5C).

## 4. Discussion

Here we explore the relationship between two well-described aspects of axon growth and regeneration – the loss of regenerative potential once development is complete and the importance of local protein synthesis in axon growth during development and in peripheral nerve injury. We show a very clear relationship between regenerative ability and local translation. Using proteomics and puromycin-based tagging of newly-synthesized proteins in combination with a novel system to assess regeneration in hESC-derived neurons, we show that regeneration in

**Table 3**
Proteins with increased levels in young axons vs aged axons.

| Proteins with increased levels in young axons vs mature axons | | | Fold change |
|---|---|---|---|
| Description | Name | Protein info | d45/ d65 |
| Phenylalanine–tRNA ligase beta subunit | FARSB | RNA translation | 8.13 |
| Insulin-like growth factor 2 mRNA-binding protein 3 | IGF2BP3 | RNA translation | 4.78 |
| Insulin-like growth factor 2 mRNA-binding protein 1 | IGF2BP1 | RNA translation, involved in axon regeneration | 3.72 |
| UDP-glucose:glycoprotein glucosyltransferase 2 | UGGT2 | Protein folding | 3.39 |
| Golgi-specific brefeldin A-resistance guanine nucleotide exchange factor 1 | GBF1 | GEF for Arf family | 3.30 |
| Extracellular sulfatase Sulf-1 | SULF1 | Heparan sulfatase | 2.83 |
| Tubulin alpha-1A chain | TUBA1A | Cytoskeleton | 2.71 |
| ATP-binding cassette sub-family D member 1 | ABCD1 | peroxisome membrane | 2.68 |
| 60S ribosomal protein L35 | RPL35 | RNA translation | 2.49 |
| Eukaryotic translation initiation factor 3 subunit C-like protein | EIF3CL | RNA translation | 2.49 |
| Peroxidasin homolog | PXDN | ECM component | 2.45 |
| Glutamine–tRNA ligase | QARS | RNA translation | 2.25 |
| Serine/threonine-protein kinase Nek9 | NEK9 | Kinase | 2.24 |
| ADP/ATP translocase 3 | SLC25A6 | Mitochondria | 2.23 |
| Catechol *O*-methyltransferase | COMT | Degradation of dopamine | 2.14 |
| 60S ribosomal protein L38 | RPL38 | RNA translation | 2.07 |
| 60S ribosomal protein L24 | RPL24 | RNA translation | 2.04 |
| Glucosylceramidase | GBA | Lysosome membrane | 1.94 |
| Neural cell adhesion molecule L1-like protein | CHL1 | ECM/membrane | 1.92 |
| Cell cycle and apoptosis regulator protein 2 | CCAR2 | nuclear, except with MCC | 1.88 |
| 26S proteasome non-ATPase regulatory subunit 7 | PSMD7 | Proteasome | 1.87 |
| Eukaryotic translation initiation factor 3 subunit B | EIF3B | RNA translation | 1.87 |
| Protein transport protein Sec61 subunit alpha isoform 1 | SEC61A1 | Secretion | 1.85 |
| cAMP-dependent protein kinase catalytic subunit alpha | PRKACA | cAMP signaling | 1.84 |
| Pyruvate kinase PKM | PKM | Glycolytic enzyme | 1.77 |
| Sortilin | SORT1 | Endocytosis | 1.77 |
| Interferon-inducible double-stranded RNA-dependent protein kinase activator A | PRKRA | RNA binding, involved in Parkinsonian dystonia | 1.77 |
| cGMP-inhibited 3′,5′-cyclic phosphodiesterase A | PDE3A | Transmembrane cAMP binding enzyme | 1.76 |
| Coronin | CORO7-PAM16 | Actin binding | 1.75 |
| Cytoskeleton-associated protein 4 | CKAP4 | Cytoskeleton | 1.71 |
| Leucine–tRNA ligase, cytoplasmic | LARS | RNA translation | 1.70 |
| Serrate RNA effector molecule homolog | SRRT | miRNA processing, nuclear/cyto shuttle | 1.70 |
| Phosphoribosylformylglycinamidine synthase | PFAS | Metabolism | 1.66 |
| Poly(rC)-binding protein 2 | PCBP2 | RNA translation | 1.66 |
| Reticulocalbin-2 | RCN2 | Interacts with Pentraxin | 1.61 |
| Polypyrimidine tract binding protein 1, isoform CRA_b | PTBP1 | Splicing factor | 1.58 |
| Dynamin-2 | DNM2 | Endocytosis | 1.57 |
| Ras-related protein Rab-30 | RAB30 | Membrane trafficking | 1.56 |
| Coatomer subunit alpha | COPA | Endocytosis | 1.53 |
| Isoleucine–tRNA ligase, cytoplasmic | IARS | RNA translation | 1.52 |

**Table 3** (*continued*)

| Proteins with increased levels in young axons vs mature axons | | | Fold change |
|---|---|---|---|
| Description | Name | Protein info | d45/ d65 |
| RNA-binding protein EWS | EWSR1 | RNA translation | 1.50 |
| C-terminal-binding protein 1 | CTBP1 | RNA translation | 1.49 |
| TIP41-like protein | TIPRL | Negative reg TOR | 1.48 |
| Nestin | NES | Neurogenesis | 1.45 |
| E3 ubiquitin-protein ligase HUWE1 | HUWE1 | Axon branching | 1.42 |
| 40S ribosomal protein S5 | RPS5 | RNA translation | 1.40 |
| Methionine–tRNA ligase, cytoplasmic | MARS | RNA translation | 1.38 |
| High density lipoprotein binding protein (Vigilin), isoform CRA_a | HDLBP | Metabolism | 1.38 |
| Exportin-2 | CSE1L | Nuclear/cyto | 1.38 |
| Surfeit 4 | SURF4 | Transmembrane | 1.35 |

Axons of in vitro hESC-derived neurons were collected at time point d45 and d65 in triplicate. Proteins were isolated from the axonal fractions and analysed using mass spectrometry. The table shows proteins that were present at increased level at d45 compared to d65.

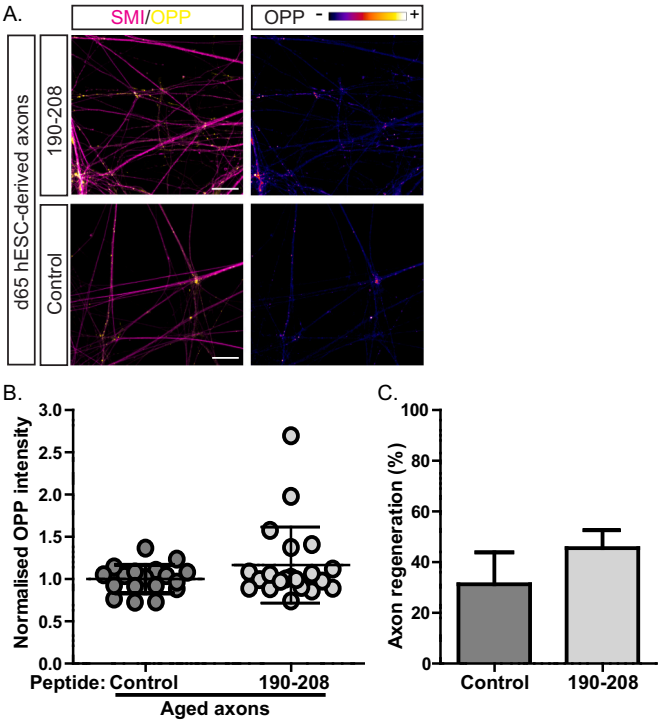


**Fig. 5.** Dominant negative G3BP1-peptide is unable to promote axonal translation or regeneration in aged hESC-derived neurons.
**A**. Immunolabeling of OPP-treated (yellow left and range indicator right) d65 hESC-derived axons (SMI312, magenta) treated with truncated G3BP1 cell permeable peptide (amino acid 190–208) in top panels and untreated control in bottom panels. Scale bar 20 μm **B**. Quantification of OPP intensity in d61-65 axons treated with 190–108 G3BP1 peptide or control. $N = 2$ experiments, 10 images per condition per experiment. $P = 0.1294$ unpaired *t*-test Welch correction. **C**. Quantification of percentage of regenerating aged axons (>d55) after laser-mediated axotomy and treated with 190–208 G3BP1 peptide or control. $N = 4$ experiments, $9 = 11$ cells per experiment. $P = 0.1839$ paired t-test.

younger axons is associated with local protein translation, as shown previously in the PNS. In older axons with diminished regenerative capacity, we show reduced local translation due, we suggest, to a reduction in the axonal levels of the protein synthesis machinery required. Together, our results provide strong evidence that, as in development and in the PNS, local translation contributes to CNS axon regeneration.

Our results suggest that an intrinsic loss of local mRNA translation capability contributes to the reduced regenerative ability of older CNS axons contrasts with work in the PNS. Here, transcriptional analysis reveals no difference in the neuronal cell body response within the DRG following sciatic nerve injury in 2 and 24 month old animals (Painter et al., 2014). These results argue against intrinsic differences between the response to the young and old neurons following injury. Rather, transplantation studies where segments of young sciatic nerve were placed into older animals post injury, or vice versa, reveal that the age of the grafted tissue determines regeneration speed. Older grafts reduce axon regrowth when placed in young animals, while young grafts placed in older animals increase axon regrowth (Painter et al., 2014; Scheib and Höke, 2016). This extrinsic effect is mediated by age-related differences in Schwann cells and macrophages, with the former failing to rapidly activate a transcriptional repair program and the latter showing reduced migration into the injured nerve (Painter et al., 2014; Scheib and Höke, 2016). Our experimental strategy clearly cannot address the question of extrinsic environmental effects in the CNS, as seen in the changes in tissue biomechanics identified as a factor in the age-related reduction in another CNS regenerative response, remyelination (Segel et al., 2019). They do however illustrate clear differences between intrinsic determinants of regenerative capacity in the CNS and the PNS as well as point to differences intrinsic to axons.

The hESC-based protocol we have used here provides an additional tool for the study of CNS regeneration that has some useful novel features. First, the use of human cells increases translational relevance. Second, the scale of axon growth observed from a central cluster of cultured neurons enable proteomics approaches to identify changes in local translation in axons as they mature, or in the axons during regeneration. Our results examining maturation showing a switch from translation-associated proteins to those associated with synaptogenesis agree well with previous work (Gumy et al., 2011; Zou et al., 2013). However, whereas axonal profiling experiments have been performed at the mRNA level, to our knowledge ours is the first study to look at newly synthesized proteins as a response to injury specifically in axons (Shigeoka et al., 2016). There are technical limitations to this experiment, as the overall rate of protein synthesis is low in axons, complicating the isolation of sufficient starting material and resulting in a low signal-to-noise level of the detection method after pulldown. In addition, the potential time window for translation of different regeneration-associated proteins is wide and our approach provides a narrow snapshot of the overall regeneration response. Nevertheless, we find robust changes that take place in the translatome of injured axons.

The largest category of proteins in the human axonal translatome is related to (lysosomal) degradation, a process that is also strongly upregulated in vivo early after injury (Springer et al., 1997). The second largest category are proteins related to translation, in keeping with the finding that newly-synthesized ribosomal proteins are incorporated into pre-existing axonal ribosomes in severed Xenopus axons (Shigeoka et al., 2019). These results underline the importance of local protein synthesis as an early process after axonal injury, representing a promising target for therapeutic approaches to enhance regeneration. Further work comparing the profile of local protein synthesis in younger (regenerative) and older (non-regenerative) axons would be valuable in identifying further targets. Within the remaining proteins in our current dataset, however, three sets of comparisons between them and with published studies on mRNAs present in normal and injured neurons and their axons reveal a small number of proteins that may also point to such targets. First, a comparison of proteins present in young (d45) axons and newly-synthesized following injury identifies LARS, MARS, IGF2BP3and HUWE1. LARS and MARS, as tRNA synthetases, are part of the core translational machinery already identified above. IGF2BP3 belongs to the IGF2BP family of mRNA binding proteins implicated in the regulation of translation of IGF2 mRNA and other transcripts including those encoding mitochondrial components. Interestingly a closely related family member IGF2BP2 is highly expressed in developing axons and binds mRNAs encoding proteins implicated in axon guidance (Preitner et al., 2016). HUWE1, by contrast, is an E3 ubiquitin ligase implicated in multiple facets of CNS development including axon development whose importance is highlighted by the findings that genetic changes cause intellectual disability and other neurodevelopmental defects in humans (Giles and Grill, 2020). Second, a comparison of our own proteomics data in young axons with the dataset generated by Shigeoka et al. (2016) using the Ribotag mouse to identify axonal mRNAs in the visual system reveals a different set of molecules comprising two proteasome subunit components PSMB4 and PSMD3, the plexin PLXNB2 implicated in neural precursor proliferation and migration (Deng et al., 2007), another ubiquitin ligase UBE2O, the GMP reductase GMPR2, AP3M1 encoding part of the AP-3 adaptor complex involved in budding from the Golgi membrane, and NAPG encoding a NSF attachment protein involved in membrane fusion and transport. Finally, a comparison with existing datasets that identified regeneration associated genes (RAG) in PNS axons (Stam et al., 2007; Costigan et al., 2010; Michaelevski et al., 2010; Geeven et al., 2011) showed little overlap with the proteins we found to be upregulated after injury; the phosphatase PHPT1 that shows increased levels in synapses tagged by C1q for pruning (Györffy et al., 2018) is the single overlapping protein that is translated in axons after injury. The lack of overlap between our data and the known RAGs may reflect the poor expression of RAGs following injury of CNS neurons and also the different time frames. Most RAGs are upregulated days to weeks after injury (van Kesteren et al., 2011; Ma and Willis, 2015), while our experiment examines the local and immediate processes that take place in injured axons.

Although our experimental approach lacks a true gain of function experiment, as we predicted that the release of sequestered mRNAs by the G3BP1 peptide would not increase regeneration given that the translation machinery was lacking in the older axons, our results do provide proof of principle that the maturation-associated reduction in translation can be reversed. We showed that the presence of OPCs can increase intrinsic axonal protein synthesis levels and promote regeneration. This argues against an irreversible cause of reduced translation efficiency in older cells eg accumulation of DNA damage. Although the beneficial effects of glia precursor cells such as OPC have been demonstrated before, the molecular mechanisms remain unclear. Our results do not distinguish whether the increase in translation in the presence of OPCs is the direct cause of enhanced regeneration, or a consequence of the OPCs generating pro-regenerative factors. Further experiments are required to explore this. In these, one focus will be secreted proteins or vesicles such as exosomes that might transfer translation-associated proteins from cell to cell, as Schwann cell exosomes were shown to promote axon regeneration in vivo (Sotelo et al., 2014; Ching and Kingham, 2015; Shakhbazau et al., 2016) and we have identified Eif3B in hOPC-isolated exosomes (S.v.E. unpublished observations). At this stage, however, we can conclude that reversing maturation-associated loss of translation represents an attractive target for strategies designed to promote CNS regeneration following axonal injury.

Supplementary data to this article can be found online at https://doi.org/10.1016/j.expneurol.2020.113594.

## Declaration of Competing Interest

The authors declare there are no competing interests.

## Acknowledgements

Grants supporting this study were EMBO ALTF1436-2015 (SvE), MS Society UK Research Grant 79 (CffC and SvE), Neurostemcellrepair FP7 (CffC), Wellcome Trust Investigator award 104783/Z/14/Z (CffC). This study was furthermore made possible by funding from National Institutes of Health to JLT (R01-NS117821) and South Carolina Spinal Cord Injury Research fund to PKS (2019-PD-02).

Alex von Kriegsheim at the IGMM Mass Spectrometry facility

(University of Edinburgh) carried out the identification of newly synthesized peptides following axonal injury, for which the "Wellcome Trust (Multiuser Equipment Grant, 208402/Z/17/Z)" was used to buy Lumos. Lisa Imrie and Dr. Thierry Le Bihan at the EdinOmics research facility at the University of Edinburgh carried out the mass spectrometry experiments and analyses on axonal samples of different ages. The authors also want to thank Tissue Culture (SCRM) and Imaging (CRM and CALM at QMRI) facility staff for their support and expertise, in particular Dr Trudi Gillespie, Dr Rachel Verdon, and Dr Bertrand Vernay.

## References

Chambers, S.M., et al., 2009. Highly efficient neural conversion of human ES and iPS cells by dual inhibition of SMAD signaling. Nat. Biotechnol. https://doi.org/10.1038/nbt.1529.

Chen, M.S., et al., 2000. Nogo-a is a myelin-associated neurite outgrowth inhibitor and an antigen for monoclonal antibody IN-1. Nature 403 (6768), 434–439. https://doi.org/10.1038/35000219.

Ching, R.C., Kingham, P.J., 2015. The role of exosomes in peripheral nerve regeneration. Neural Regen. Res. 10 (5), 743–747. https://doi.org/10.4103/1673-5374.156968.

Costigan, M., et al., 2010. Multiple chronic pain states are associated with a common amino acid–changing allele in KCNS1. Brain 133 (9), 2519–2527. https://doi.org/10.1093/brain/awq195.

Deng, S., et al., 2007. Plexin-B2, but not plexin-B1, critically modulates neuronal migration and patterning of the developing nervous system in vivo. J. Neurosci. https://doi.org/10.1523/JNEUROSCI.5381-06.2007.

Eva, R., Andrews, M.R., Franssen, E.H.P., 2012. Intrinsic mechanisms regulating axon regeneration: an integrin perspective. Int. Rev. Neurobiol. 106, 75–104. https://doi.org/10.1016/B978-0-12-407178-0.00004-1.

Fawcett, J.W., Verhaagen, J., 2018. Intrinsic determinants of axon regeneration. Dev. Neurobiol. 78 (10), 890–897. https://doi.org/10.1002/dneu.22637.

Fawcett, J.W., et al., 2012. Defeating inhibition of regeneration by scar and myelin components. Handb. Clin. Neurol. 109, 503–522. https://doi.org/10.1016/B978-0-444-52137-8.00031-0.

Geeven, G., et al., 2011. LLM3D: a log-linear modeling-based method to predict functional gene regulatory interactions from genome-wide expression data. Nucleic Acids Res. 39 (13), 5313–5327. https://doi.org/10.1093/nar/gkr139.

Geoffroy, C.G., Zheng, B., 2014. Myelin-associated inhibitors in axonal growth after CNS injury. Curr. Opin. Neurobiol. 27, 31–38. https://doi.org/10.1016/j.conb.2014.02.012.

Giles, A.C., Grill, B., 2020. Roles of the HUWE1 ubiquitin ligase in nervous system development, function and disease. Neural Dev. https://doi.org/10.1186/s13064-020-00143-9.

Gumy, L.F., et al., 2011. Transcriptome analysis of embryonic and adult sensory axons reveals changes in mRNA repertoire localization. RNA 17 (1), 85–98. https://doi.org/10.1261/rna.2386111.

Gumy, L.F., et al., 2014. New insights into mRNA trafficking in axons. Dev. Neurobiol. 74 (3), 233–244. https://doi.org/10.1002/dneu.22121.

Györffy, B.A., et al., 2018. Local apoptotic-like mechanisms underlie complementmediated synaptic pruning. Proc. Natl. Acad. Sci. U. S. A. https://doi.org/10.1073/pnas.1722613115.

Haas, C., Fischer, I., 2013. Human astrocytes derived from glial restricted progenitors support regeneration of the injured spinal cord. J. Neurotrauma 30 (12), 1035–1052. https://doi.org/10.1089/neu.2013.2915.

Hayakawa, K., et al., 2015. Glial restricted precursors maintain their permissive properties after long-term expansion but not following exposure to pro-inflammatory factors. Brain Res. 1629, 113–125. https://doi.org/10.1016/j.brainres.2015.10.022.

Hayakawa, K., Haas, C., Fischer, I., 2016. Examining the properties and therapeutic potential of glial restricted precursors in spinal cord injury. Neural Regen. Res. 11 (4), 529–533. https://doi.org/10.4103/1673-5374.180725.

Ji, S.-J., Jaffrey, S.R., 2013. Axonal transcription factors: novel regulators of growth cone-to-nucleus signaling. Dev. Neurobiol. 74 (3), 245–258. https://doi.org/10.1002/dneu.22112.

Jin, Y., Shumsky, J.S., Fischer, I., 2018. Axonal regeneration of different tracts following transplants of human glial restricted progenitors into the injured spinal cord in rats. Brain Res. 1686, 101–112. https://doi.org/10.1016/j.brainres.2018.01.030.

Kar, A.N., Lee, S.J., Twiss, J.L., 2017. Expanding axonal Transcriptome brings new functions for Axonally synthesized proteins in health and disease. Neuroscientist. https://doi.org/10.1177/1073858417712668, 107385841771266.

Keirstead, H.S., et al., 2005. Human embryonic stem cell-derived oligodendrocyte progenitor cell transplants remyelinate and restore locomotion after spinal cord injury. J. Neurosci. 25 (19), 4694–4705. https://doi.org/10.1523/JNEUROSCI.0311-05.2005.

Kirkeby, A., et al., 2012. Generation of regionally specified neural progenitors and functional neurons from human embryonic stem cells under defined conditions. Cell Rep. 1 (6), 703–714. https://doi.org/10.1016/j.celrep.2012.04.009.

Koseki, H., et al., 2017. Selective rab11 transport and the intrinsic regenerative ability of CNS axons. eLife 6. https://doi.org/10.7554/eLife.26956.

Li, D., Field, P.M., Raisman, G., 1995. Failure of axon regeneration in postnatal rat Entorhino-hippocampal slice Coculture is due to maturation of the axon, not that of the pathway or target. Eur. J. Neurosci. 7 (6), 1164–1171. https://doi.org/10.1111/j.1460-9568.1995.tb01106.x.

Livesey, M.R., et al., 2016. Maturation and electrophysiological properties of human pluripotent stem cell-derived oligodendrocytes. Stem Cells 34 (4), 1040–1053. https://doi.org/10.1002/stem.2273.

Ma, T.C., Willis, D.E., 2015. What makes a RAG regeneration associated? Front. Mol. Neurosci. https://doi.org/10.3389/fnmol.2015.00043.

Mi, H., et al., 2013. Large-scale gene function analysis with the PANTHER classification system. Nat. Protoc. 8 (8), 1551–1566. https://doi.org/10.1038/nprot.2013.092.

Michaelevski, I., et al., 2010. Signaling to transcription networks in the neuronal retrograde injury response. Sci. Signal. 3 (130) https://doi.org/10.1126/scisignal.2000952 ra53-ra53.

Michalski, A., et al., 2011. Mass spectrometry-based proteomics using Q exactive, a high-performance benchtop quadrupole orbitrap mass spectrometer. Mol. Cell. Proteomics 10 (9). https://doi.org/10.1074/mcp.M111.011015. M111.011015.

Nieuwenhuis, B., et al., 2020. PI 3-kinase delta enhances axonal PIP 3 to support axon regeneration in the adult CNS. EMBO Mol. Med. https://doi.org/10.15252/emmm.201911674.

Pacheco, A., et al., 2020. Mechanism and role of the intra-axonal Calreticulin translation in response to axonal injury. Exp. Neurol. https://doi.org/10.1016/j.expneurol.2019.113072.

Painter, M.W., et al., 2014. Diminished Schwann cell repair responses underlie age-associated impaired axonal regeneration. Neuron. https://doi.org/10.1016/j.neuron.2014.06.016.

Preitner, N., et al., 2016. IMP2 axonal localization, RNA interactome, and function in the development of axon trajectories. Development (Cambridge). https://doi.org/10.1242/dev.128348.

Prinjha, R., et al., 2000. Inhibitor of neurite outgrowth in humans. Nature 403 (6768), 383–384. https://doi.org/10.1038/35000287.

Sahoo, P.K., et al., 2018. Axonal G3BP1 stress granule protein limits axonal mRNA translation and nerve regeneration. Nat. Commun. 9 (1), 3358. https://doi.org/10.1038/s41467-018-05647-x.

Sahoo, P.K., et al., 2020. A $Ca^{2+}$-dependent switch activates axonal casein kinase 2α translation and drives G3BP1 granule disassembly for axon regeneration. Curr Biol. 30 (24), 4882–4895. https://doi.org/10.1016/j.cub.2020.09.043. Epub 2020 Oct 15.

Scheib, J.L., Höke, A., 2016. An attenuated immune response by Schwann cells and macrophages inhibits nerve regeneration in aged rats. Neurobiol. Aging. https://doi.org/10.1016/j.neurobiolaging.2016.05.004.

Segel, M., et al., 2019. Niche stiffness underlies the ageing of central nervous system progenitor cells. Nature. https://doi.org/10.1038/s41586-019-1484-9.

Shakhbazau, A., et al., 2016. Demyelination induces transport of ribosome-containing vesicles from glia to axons: evidence from animal models and MS patient brains. Mol. Biol. Rep. 43 (6), 495–507. https://doi.org/10.1007/s11033-016-3990-2.

Sharp, J., et al., 2010. Human embryonic stem cell-derived oligodendrocyte progenitor cell transplants improve recovery after cervical spinal cord injury. Stem Cells (Dayton, Ohio) 28 (1), 152–163. https://doi.org/10.1002/stem.245.

Shigeoka, T., et al., 2016. Dynamic axonal translation in developing and mature visual circuits. Cell 166 (1), 181–192. https://doi.org/10.1016/j.cell.2016.05.029.

Shigeoka, T., et al., 2019. On-site ribosome Remodeling by locally synthesized ribosomal proteins in axons. Cell Rep. https://doi.org/10.1016/j.celrep.2019.11.025.

Smith, C.L., et al., 2004. GAP-43 mRNA in growth cones is associated with HuD and ribosomes. J. Neurobiol. https://doi.org/10.1002/neu.20038.

Sotelo, J.R., et al., 2014. Glia to axon RNA transfer. Dev. Neurobiol. 74 (3), 292–302. https://doi.org/10.1002/dneu.22125.

Springer, J.E., et al., 1997. Rapid Calpain I activation and cytoskeletal protein degradation following traumatic spinal cord injury: attenuation with Riluzole Pretreatment. J. Neurochem. 69 (4), 1592–1600. https://doi.org/10.1046/j.1471-4159.1997.69041592.x.

Stam, F.J., et al., 2007. Identification of candidate transcriptional modulators involved in successful regeneration after nerve injury. Eur. J. Neurosci. https://doi.org/10.1111/j.1460-9568.2007.05597.x.

Terenzio, M., et al., 2018. Locally translated mTOR controls axonal local translation in nerve injury. Science 359 (6382), 1416–1421. https://doi.org/10.1126/science.aan1053.

Turriziani, B., et al., 2014. On-beads digestion in conjunction with data-dependent mass spectrometry: a shortcut to quantitative and dynamic interaction proteomics. Biology. https://doi.org/10.3390/biology3020320.

van Kesteren, R.E., et al., 2011. A gene network perspective on axonal regeneration. Front. Mol. Neurosci. https://doi.org/10.3389/fnmol.2011.00046.

Verma, P., et al., 2005. Axonal protein synthesis and degradation are necessary for efficient growth cone regeneration. J. Neurosci. 25 (2), 331–342. https://doi.org/10.1523/JNEUROSCI.3073-04.2005.

Zheng, J.Q., et al., 2001. A functional role for intra-axonal protein synthesis during axonal regeneration from adult sensory neurons. J. Neurosci. 21 (23), 9291–9303. Available at. http://www.ncbi.nlm.nih.gov/pubmed/11717363 (Accessed: 6 March 2017).

Zou, Y., et al., 2013. Developmental decline in neuronal regeneration by the progressive change of two intrinsic timers. Science (New York, N.Y.) 340 (6130), 372–376. https://doi.org/10.1126/science.1231321.